

<https://helda.helsinki.fi>

---

## Molecular dynamics simulations of ballistic He penetration into W fuzz

Klaver, T. P. C.

2016-12

---

Klaver , T P C , Nordlund , K , Morgan , T W , Westerhof , E , Thijsse , B J & van de Sanden  
, M C M 2016 , ' Molecular dynamics simulations of ballistic He penetration into W fuzz ' ,  
Nuclear Fusion , vol. 56 , no. 12 , 126015 . <https://doi.org/10.1088/0029-5515/56/12/126015>

---

<http://hdl.handle.net/10138/308225>

<https://doi.org/10.1088/0029-5515/56/12/126015>

---

cc\_by\_nc\_nd

acceptedVersion

---

*Downloaded from Helda, University of Helsinki institutional repository.*

*This is an electronic reprint of the original article.*

*This reprint may differ from the original in pagination and typographic detail.*

*Please cite the original version.*

(published, T.P. C. Klaver *et al*, Nucl. Fusion 56 (2016) 126015)

## Molecular dynamics simulations of ballistic He penetration into W fuzz

T. P. C. Klaver<sup>1, 2\*</sup>, K. Nordlund<sup>3</sup>, T. W. Morgan<sup>1</sup>, E. Westerhof<sup>1</sup>, B. J. Thijsse<sup>2</sup>, M. C. M. van de Sanden<sup>1</sup>

<sup>1</sup> FOM Institute DIFFER - Dutch Institute for Fundamental Energy Research,  
Partner in the Trilateral Euregio Cluster, Eindhoven, The Netherlands

<sup>2</sup> Department of Materials Science and Engineering, Delft University of Technology,  
Delft, The Netherlands

<sup>3</sup> Association EURATOM-Tekes – Department of Physics, University of Helsinki,  
Finland

### Abstract

Results are presented of large-scale Molecular Dynamics simulations of low-energy He bombardment of W nanorods, or so-called “fuzz” structures. The goal of these simulations is to see if ballistic He penetration through W fuzz offers a more realistic scenario for how He moves through fuzz layers than He diffusion through fuzz nanorods. Instead of trying to grow a fuzz layer starting from a flat piece of bulk W, a new approach of creating a fully formed fuzz structure 0.43  $\mu\text{m}$  thick out of ellipsoidal pieces of W is employed. Lack of detailed experimental knowledge of the three-dimensional structure of fuzz is dealt with by simulating He bombardment on five different structures of 15vol% W and determining the variation in He penetration for each case. The results show that by far the most important factor determining He penetration is the amount of open channels through which He ions can travel unimpeded. For a more or less even W density distribution He penetration into fuzz falls off exponentially with distance and can thus be described by a ‘half depth’. In a 15 vol% fuzz structure, the half depth can reach 0.18  $\mu\text{m}$ . In the far sparser fuzz structures that were recently reported, the half depth might be 1  $\mu\text{m}$  or more. This means that ballistic He penetration offers a more likely scenario than He diffusion through nanorods for how He moves through fuzz and may provide an adequate explanation for how He penetrates through the thickest fuzz layers reported so far. Furthermore, the exponential decrease in penetration with depth would follow a logarithmic dependence on fluence which is compatible with experiments. A comparison of these results and molecular dynamics calculations carried out in the recoil interaction approximation shows that results for W fuzz are qualitatively very different from conventional stopping power calculations on W with a similarly low but homogeneous density distribution.

### 1 Introduction

The W divertor in the ITER fusion tokamak being built in France will be subjected to intense bombardment by low energy ions, including He, the ash of the fusion reaction. In 2006 Takamura *et al* [1] first reported that intense low energy He bombardment from a fusion plasma (simulated in a linear plasma

device) can transform a solid W surface into a very open, low density 'fuzz', raising concerns about the thermal properties and cohesion of such structures. Since then W fuzz layers [2-28], as well as fuzz layers on other metals [12, 15, 29] have been an active area of research. Not all details of the formation process are fully known yet, but a number of observations are commonly made. Baldwin and Doerner [3] observed that fuzz layer thickness develops with the square root of the exposure time. This pattern was found in other investigations too [5, 7, 12, 26], albeit sometimes with minor modifications. It was found [5, 7, 26] that fuzz growth may not start immediately but after an incubation or saturation time instead. Also, in experiments with different He fluxes, results show closest agreement with each other when interpreted in terms of their total fluence rather than exposure time [26]. Reports of fuzz growth are often accompanied by the observation of pinholes in the surface and He bubble formation. Bubbles form both right under the fuzz layer just above the still unaffected W bulk, as well as inside the thin nanorods [12, 2, 7, 15, 22] that make up the fuzz. Kajita *et al* [4, 7] have presented a model for how fuzz forms in which pinholes and He bubble formation, growth, migration, coalescence and bursting at surfaces play a key role. Recently, Takamu and Uesugi [27] showed W arches to be an intermediate stage between W surfaces with holes (created by burst He bubbles) and fully formed fuzz.

The square root of He dose vs. fuzz thickness pattern is reminiscent of the textbook diffusion-limited model in thin film growth in which one of the species needed to grow the film needs to diffuse through the growing film. In this model, the film grows 'from the bottom' and diffusion happens more slowly as the film grows thicker, resulting in the square root thickness pattern. Baldwin and Doerner have interpreted their findings in terms of this model and suggested that one of the processes involved is He diffusing through the fuzz nanorods to reach the W bulk, which it then proceeds to turn into more fuzz [3]. Given the low density of fuzz compared to bulk W, fuzz grows out from the original surface to accommodate the higher volume of the fuzz. He is supposed to penetrate into the W only in the outer few tens of nm of the fuzz, despite its ~90% porosity, with most of the He transport then being provided by diffusion. However, it seems unlikely that much He would still reach the bulk W by diffusion through the nanorods once the fuzz thickness has reached several micrometers. Most He would likely move near a surface at some point and desorb back to the vacuum. The issues with the above interpretation are discussed in greater detail in Appendix A.

Kajita *et al* have speculated [4, 7] whether He ions might penetrate through pinholes and possibly even through several hundred nanometers of fuzz. Given that fuzz structures can develop to be more than 90% open space rather than W, the idea of ballistic penetration of He ions into fuzz could offer a more realistic mechanism for He to reach the fuzz-bulk boundary than diffusion of interstitial He through the fuzz nanorods. The main aim of this work is to see if this is indeed the case. For this, large-scale classical molecular dynamics (MD) simulations were carried out to study how deep He ions, accelerated to relatively low kinetic energy, penetrate into W fuzz structures. Results show that ballistic He penetration into W fuzz plays a bigger role than hitherto assumed.

The structure of this paper is as follows. In section 2 the approach on how the fuzz structures were created for the ion bombardment simulations based on the

limited insight from TEM micrographs and porosity measurements is described. In section 3 computational details of the calculations are given and in section 4 results are presented. First classical MD results of He bombardment of fuzz structures are presented. These are then compared to simpler recoil approximation calculations for systems with a similar overall, but homogeneous density. In section 5 the implications of the findings are discussed and finally in section 6 a summary is given and the conclusions and directions for future work are presented.

## 2 Creating fuzz structures for He ion bombardment simulations

Simulating He ion bombardment on fuzz with classical MD requires having an atom by atom description of a fuzz structure. At present, atomistic simulation can only reproduce the very earliest stages of fuzz formation (see e.g. the recent work by Ito *et al* [30]) and falls well short of starting from flat, defect-free W and simulating its transformation into micrometer thick fuzz.

An alternative to trying to grow a fuzz structure in a simulation is to create a fully formed fuzz structure, based on data from experiments. However, this approach also poses some challenges. Experimental data on the local structure of fuzz comes primarily in the form of electron microscopy images. These provide some information like nanorod thickness (10-50 nm, possibly a bit thicker near the bulk) [3, 7, 12, 4, 1, 28] and the spacing between nanorods, but they do not provide a full three-dimensional structure of fuzz. Some further experimental information is provided by porosity measurements. However, there are still many ways to construct fuzz structures in a simulation that have the right porosity and nanorod thickness, yet most of these structures would not be similar to fuzz structures found in experiments.

The problem of creating a fuzz structure based on limited knowledge was dealt with by varying certain parameters in how fuzz is created, to arrive at a series of different fuzz structures. All these different structures were then bombarded with He to see how much He penetration differs between them. If a particular variation of the fuzz has little or no influence on He penetration, then the details of that variation are not important here and it makes no difference that it is not known which fuzz variant is closest to experiments. For fuzz parameter variations that do have an influence on He penetration it is also unknown which result is closest to experiments, but the variation in the results can be taken as the error bar associated with the variation of that parameter.

Five different fuzz structures were constructed. The first structure was made out of 90 (partly overlapping) ellipsoids. Ellipsoids were chosen as building blocks because they have rounded surfaces and are elongated in one direction, like parts of the fuzz nanorods, though other shapes would meet these criteria too. First ellipsoid dynamics were conducted in a fully periodic box in which each ellipsoid was a single hard body. Ellipsoids started on a regular 3 x 3 x 10 grid (the size of the third dimension defines the fuzz thickness, see next) and were allowed to move until no correlation to the initial ordered structure was left. Then the periodic boundary condition in the long direction was removed and some extra open space was added at the top and bottom of the system. Each ellipsoid body was replaced by a larger ellipsoid shaped piece of a bcc W crystal,



20 nm wide (near the lower limit of nanorod thickness) and 63 nm long, with the same orientation as the single body ellipsoids. If ‘atomic ellipsoids’ overlapped, the atoms of one of the ellipsoids in the overlapping volume were removed. The ellipsoids formed a mixture of overlapping and completely free ellipsoids. In each separate body of ellipsoids (either a completely free single ellipsoid or a group of ellipsoids attached to each other) the positions of a few atoms were locked in place and excluded from the normal atomic dynamics. These fixed atoms prevent the different bodies of single or clustered ellipsoids from drifting. The resulting fuzz structure is shown in fig. 1.

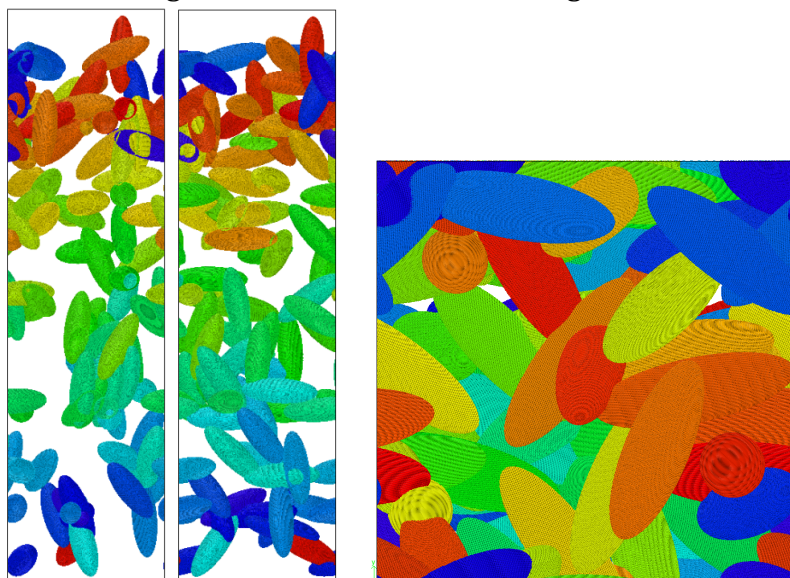


Fig. 1. Side (left), front (middle) and top (right) views of a fuzz structure created out of 90 ellipsoids built out of W atoms. See text for more details of the fuzz structure. Colours are used only to distinguish ellipsoids and do not signify any physical property.

The first variation of the ‘original’ fuzz structure above consisted of running the ellipsoid dynamics 10 times longer, so that ellipsoid positions are different. This is akin to looking at two different points of one homogeneous fuzz film. The overall properties like W density, ellipsoid thickness and angular distribution of the ellipsoids are similar, but the local arrangement of the ellipsoids is different. This is a ‘natural’ variation that could always occur between different places in a fuzz layer and it sets the size for what can be considered a small influence on He penetration. Any variation of the fuzz that is said to be significant should make a greater difference in He penetration than the difference stemming from just the local rearrangement of the ellipsoids.

In the second fuzz variation, the angles between the long axes of the ellipsoids and the surface normal of the fuzz in the original system were reduced by half. This produces a degree of texturing in the fuzz and creates more open channels that He ions can pass through unimpeded, see fig. 2. This system is hereafter referred to as ‘the textured system’.

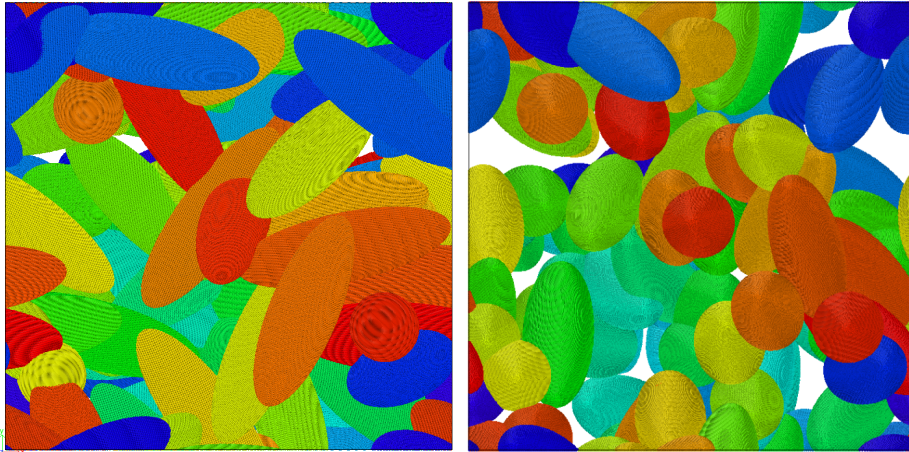


Fig. 2. Top views of the original (left) and textured (right) ellipsoid structures.

The variation with texture was chosen because some fuzz images show a preference of the nanorods to run more perpendicular to the fuzz surface than parallel to it, with open channels in between. An example of this is shown in figure 3, but can also be observed in e.g. fig. 14c in [31], fig. 4a in [4] or fig. 4b in [7]. This can obviously be expected to lead to deeper He penetration.

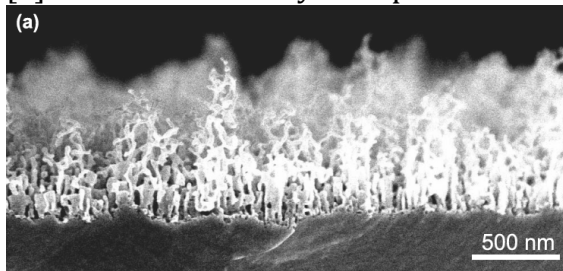


Fig. 3. Image of W fuzz showing preferential orientation of nanorods perpendicular to the surface. Reproduced from [15] with permission.

The third variation consisted of building a fuzz structure out of dumbbells (also 20 nm wide and 63 nm long, positions and orientations similar to those of the ellipsoids in the original system) rather than ellipsoids. This was done because some fuzz images show nanorod ends not gradually thinning into a tip but widening into a small sphere instead. An example of this is shown in figure 4, but can also be observed in e.g. fig. 5a in [12], fig. 2c in [16] or fig. 3d in [21]. Replacing ellipsoids by dumbbells would show the influence of this shape effect.

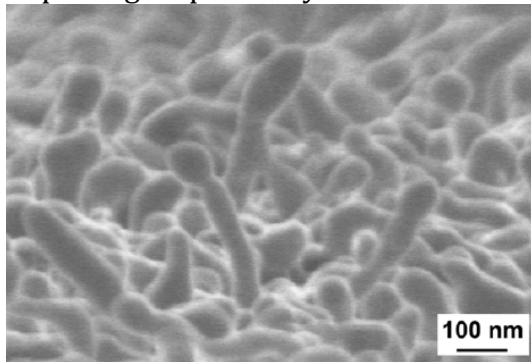


Fig. 4. Image of W fuzz showing nanorod ends widening first, rather than gradually thinning into a sharp tip. Reproduced from [4] with permission.

Since fuzz surfaces may not always be as smooth as the ellipsoid or dumbbell surfaces in previous system, a fifth fuzz variation was created to study the effect of surface roughness. This was done by changing the smooth ellipsoid surface to a one with many steps in surface height and some sharp points. This was achieved by taking two concentric ellipsoids with slightly different radii and letting the W atoms reach up to the surface of the inner ellipsoid in some parts and to the surface of the outer ellipsoid in other parts. Positions and orientations of the rough surface ellipsoids were kept similar to those in the original system. Fig. 5 shows the five different fuzz structures and their unit building blocks. More detail about the fuzz structures is given in the computational details section.

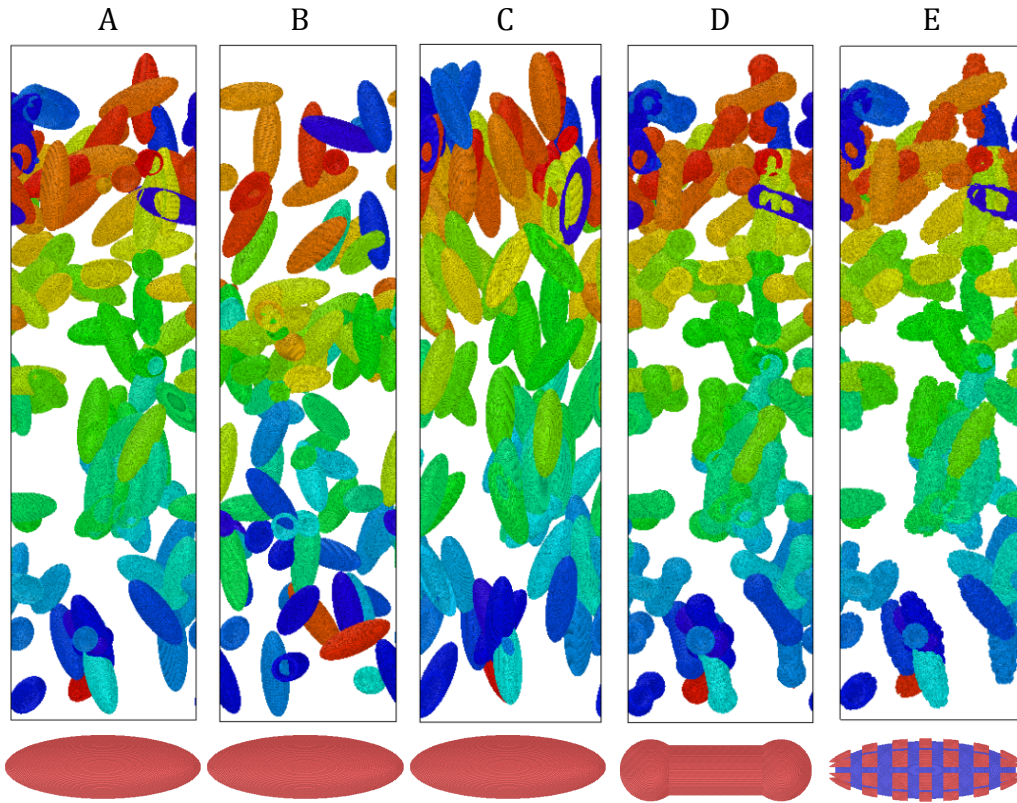


Fig. 5. Fuzz structures used in He bombardment simulations and their unit building blocks. A: original ellipsoid structure. B: ellipsoid structure with different local structure. C: textured ellipsoid structure. D: dumbbell structure. E: ellipsoid structure with rough surface. See text for more details of the fuzz structures.

### 3 Computational details

MD calculations were carried out using the open source MD code LAMMPS [32]. The Juslin-Wirth W-He potential [33] was used without explicitly taking electronic stopping into account. Periodic in-plane dimensions for all systems are fixed at  $0.13 \times 0.13 \mu\text{m}^2$ . The fuzz thickness is  $0.43 \mu\text{m}$ . These dimensions are sufficiently thick to let He lose most of its kinetic energy while moving through the fuzz and sufficiently wide to contain several ellipsoid or dumbbell widths or lengths. The thickness direction of the systems is non-periodic and allows for the removal of reflected He atoms at the top and transmitted He atoms at the bottom.



The numbers of atoms in a solid ellipsoid and dumbbell are 809881 and 840685, respectively. Since He only reflects off surfaces of nanorods (possibly after penetrating a few nm into the surface first) or thermalizes within the first few nm, ellipsoids and dumbbells can be hollowed out to reduce the number of atoms in the calculation and reduce computing time. Atoms inside shells 2 nm thick or more were removed to reduce the numbers of atoms for ellipsoids and dumbbells to 395506 and 373824, respectively. A 2 nm shell thickness was chosen because calculations (not reported in further detail here) showed that very few He atoms that penetrated 2 nm deep into W would reach the surface again and desorb from it with significant kinetic energy. Hollow ellipsoids and dumbbells are shown in fig. 6.

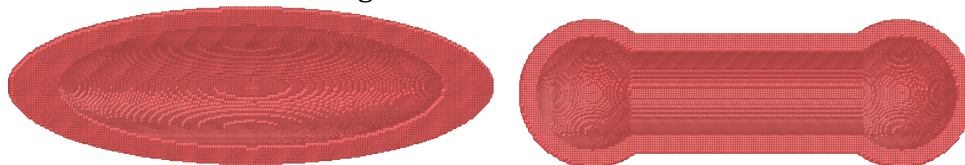


Fig. 6. Hollow ellipsoid and dumbbell unit building blocks used to create fuzz structures.

Table I lists some properties for the five fuzz structures. The open channels percentage is defined as the fraction of the fuzz structure along the thickness direction in which there is no W at all.

Table I. Properties of the five fuzz structures used in simulations.

structure	ellipsoid/ dumbbell orientation	number of atoms ( $10^6$ )	vol% W, solid structures	% open channels
A: ellipsoids, 'original'	from ellipsoid dynamics	solid: 67.1 hollow: 33.8	15.2	0.4
B: ellipsoids, different local structure	from extended ellipsoid dynamics	solid: 65.5 hollow: 33.4	14.9	0.1
C: ellipsoids, textured	From ellipsoid dynamics, then angle between surface normal and long axes of ellipsoids halved	solid: 67.9 hollow: 34.1	15.4	4.7
D: dumbbells	from ellipsoid dynamics	solid: 68.9 hollow: 32.1	15.7	0.4
E: ellipsoids, rough	from ellipsoid dynamics	solid: 64.4 hollow: 37.1	14.6	0.2

While the overall density for all systems is  $\sim 15$  vol%, the density distributions are not similar for simulation B compared to the others. Fig. 7 shows the density over the fuzz thickness, for the original ellipsoids system and the ellipsoid structure with a different local structure, in slices of  $1/20^{\text{th}}$  of the fuzz thickness.

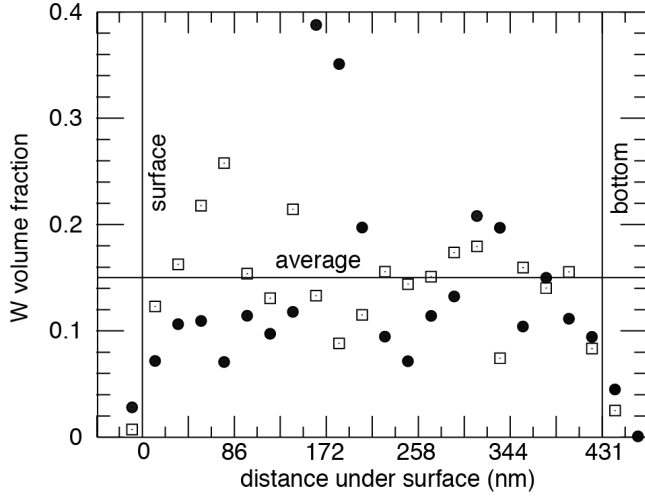


Fig. 7. Density of the original ellipsoid system (open squares) and ellipsoid system with different local structure (solid circles). W density that extends from the surface and bottom comes from ellipsoids that have their centre of mass inside the surface and bottom, but partly extend outside them.

Each fuzz structure was bombarded with 10000 He ions with kinetic energies around 59 eV, close to the energy used in [3]. He ions were introduced some distance above the highest part of the fuzz structures. Initial He velocities were mostly perpendicular to the fuzz surface. The small kinetic energy range resulted from giving He ions additional small, random in-plane velocities, making the introduction angle  $0$  to  $7.1^\circ$  off-normal. A variable time step was used so that the fastest atom in the system did not move more than  $0.025 \text{ \AA}$ , resulting in time steps of  $\sim 0.047 \text{ fs}$  during ion bombardment. As is typical for ion bombardment or deposition MD simulations, the flux ( $\sim 10^{30} \text{ m}^{-2}\text{s}^{-1}$ ) was orders of magnitude higher than in experiments, to keep down computing time. Despite the number of He atoms simultaneously present in the simulations being unrealistically high, it was verified that ‘mid air’ collisions between free He atoms were negligible (observed once). The single occurrence of such an event for a total of 50000 introduced He ions means that short-time results like ballistic penetration can be studied realistically despite the unrealistically high He flux. However, simulating longer timescale phenomena like diffusion and clustering of thermalized He inside W is not feasible in the molecular dynamics simulations due to computer time limitations. After the introduction of the last He ion, each system was allowed to evolve for a sufficiently long time for almost all He atoms to have either reflected or transmitted from the system or to have lost most of their kinetic energy while still inside the system. For all He atoms in the system, positions, velocities, forces, and potential and kinetic energies were saved for analysis every 100 steps. Information for W atoms is not saved frequently. Visualisation was done using Ovito [34].

A Nose-Hoover thermostat with a temperature damping time of 1 ps was used to keep the system temperature at 1500 K, which is in the middle of the  $\sim 1000$ -2000 K temperature range in which W fuzz grows. The W lattice parameter used to create the initial fuzz structures corresponded to the simulated W lattice parameter at 1500 K.

The calculations are sizeable by the standard of today's computing power. Running on a few nodes totalling some dozens of cpu cores, the calculations took several months to complete. It was checked if the ion range distributions in the fuzz as described in section 4 could also be obtained from conventional stopping power calculations at a tiny fraction of the computational cost. For this, molecular dynamics calculations in the recoil interaction approximation were carried out, using the MDRANGE code [35]. In this approach the lattice atom interactions are not treated, in order to achieve fast calculation of ion ranges [35]. This approach has been shown to give a very good description of ion ranges both in channeling and 'random' ion implantation directions [36-38]. The He-W interactions were described with the universal ZBL repulsive potential [38]. Since the electronic stopping is very weak (or possible even zero) at these low ion energies [39], electronic stopping was not included in the calculations (consistent with the LAMMPS simulations). Since the W fuzz material is so strongly underdense, simulations were carried out not only for regular W, but also for crystalline W with an enlarged lattice parameter and a random W atom arrangement, the latter two both at 14% of the regular density as in the lammps calculations.

## 4 Results

### 4.1 Categorising He trajectories

He ions that are inserted into the system can do one of the following:

- reflect (move back to the vacuum with high kinetic energy)
- outgas from the top of the system (move back to the vacuum with low kinetic energy)
- thermalize inside W
- thermalize inside an ellipsoid or dumbbell cavity
- keep moving freely through system with high kinetic energy
- keep moving freely through system with low kinetic energy
- transmit (pass through the system with high kinetic energy)
- outgas from the bottom of the system (pass through the system with low kinetic energy)

Since the cavities are artificial constructs, He atoms that end up in cavities are considered as having thermalized inside W. The dividing energy between high and low kinetic energy was set at the W surface barrier for He, which is  $\sim 8$  eV, see appendix B.

Analysis of what happened to He ions was mostly automated by looking at either the last recorded stage in the trajectory, the last 10 stages (covering 1000 MD steps) or the last 3000 stages (covering 300000 MD steps). The analysis criteria and full details on how these were determined are given in appendix B. Table 2 and fig. 8 show what happened to the He ions for different fuzz structures.

Table 2. Percentages of He atoms in different categories at the end of simulations. The errors in the data were determined by taking the percentages for the first and second halves of all He atoms and seeing how far these deviate from the average over all ions.

category	ellipsoids, original	ellipsoids, different local structure	ellipsoids, textured	Dumbbells	ellipsoids, rough surface
reflected	42.3±0.1	42.1±0.4	30.0±0.5	43.7±0.0	43.3±0.1
outgassed, top	9.7±0.1	10.2±0.1	9.0±0.0	10.4±0.1	10.8±0.1
thermalized	25.2±0.2	26.2±0.1	22.1±0.3	21.5±0.2	25.6±0.0
inside cavity	5.1±0.2	4.9±0.0	3.6±0.0	8.1±0.0	3.6±0.0
free, $E_k > 8$ eV	0.1±0.0	0.0±0.0	0.0±0.0	0.2±0.0	0.0±0.0
free, $E_k < 8$ eV	7.2±0.1	7.4±0.3	7.1±0.1	7.6±0.1	7.4±0.2
outgassed, bottom	3.0±0.0	2.5±0.1	4.9±0.0	2.8±0.2	3.2±0.0
transmitted	7.5±0.0	6.7±0.2	23.3±0.4	5.8±0.0	6.1±0.0

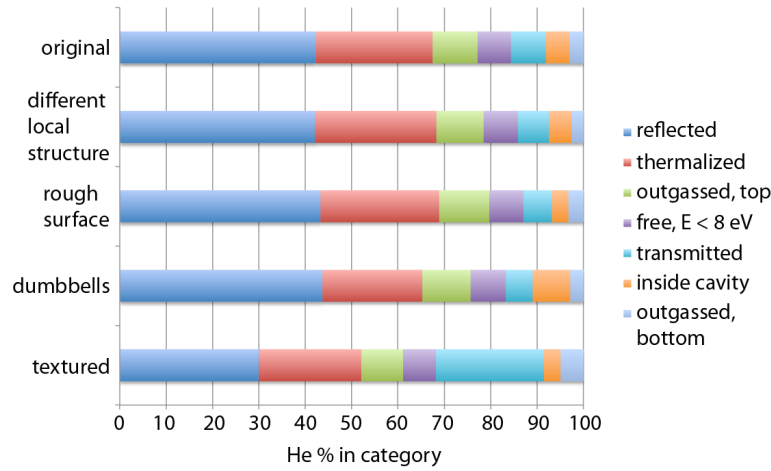


Fig. 8. Percentages of He in different categories at the end of simulations.

The percentage of He atoms inside dumbbell cavities is higher than inside ellipsoid cavities because dumbbell shells are 2 nm thick everywhere while ellipsoid shells vary between 2 and 6.3 nm. Fig. 9 shows a few examples of He trajectories.

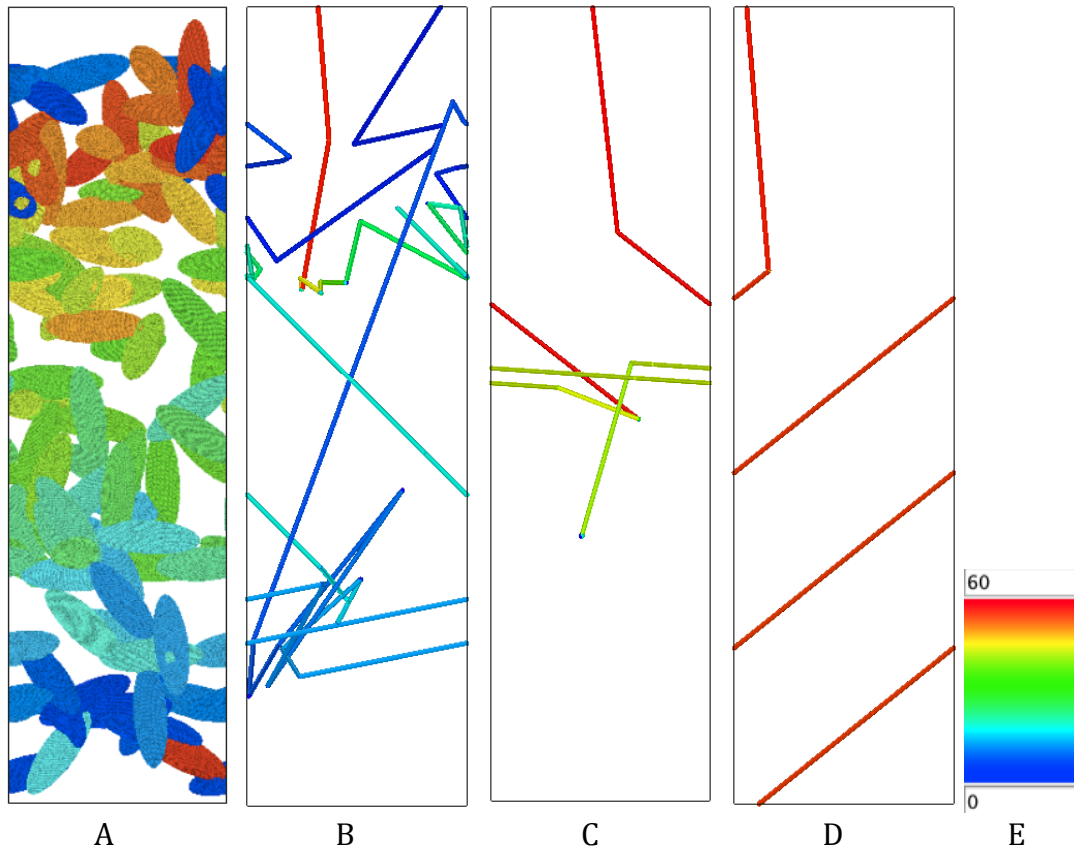


Fig. 9. Examples of He trajectories through fuzz. Trajectories are coloured according to the kinetic energy of the He atoms. A: the fuzz structure. B: He atom loses kinetic energy as it bounces off many W surfaces, outgasses back to the open vacuum with low kinetic energy. C: On its fifth impact with a W surface, a He atom penetrates into W, thermalizes and becomes embedded as an interstitial inside W. D: with a single bounce off a W surface, He transmits through the system with most of its kinetic energy. E: He kinetic energy colour scale (eV).

In the next sections the He atoms in some of the categories are analysed in more detail.

#### 4.2 Kinetic energy of free He moving through fuzz

To see how deep He penetrates, the 'penetrative power' left among the He atoms as a function of penetration depth is investigated. Penetrative power should be a measure for how much deeper He can be expected to penetrate into the fuzz.

Here it is taken (pragmatically, other definitions are possible) to be the sum of the kinetic energies of He atoms that adhere to the following criteria:

- 1) the atom is moving through open space all or most of the time (not embedded inside W or inside a cavity)
- 2) the atom is moving deeper into the fuzz, not moving back to the open vacuum
- 3) the atom has at least 8 eV of kinetic energy (so that it could still penetrate the W surface barrier for He and become embedded in W)

The result is shown in fig. 10, normalized relative to the penetrative power at a penetration depth of 0 nm.



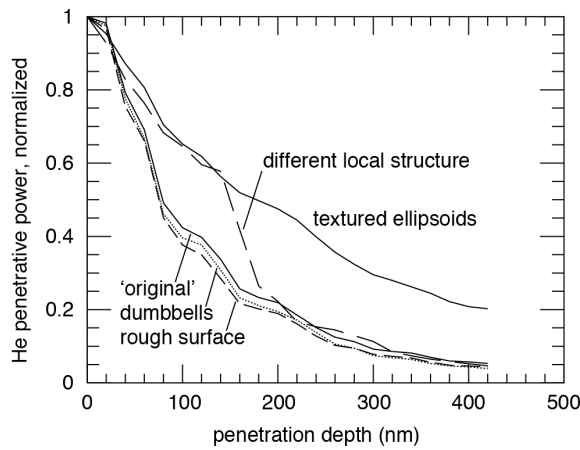


Fig. 10. Normalized He penetrative power as a function of penetration depth for the five fuzz structures.

From fig. 10 it is clear that surface roughness and the unit building block of the structure have little influence while the amount of open channels through texturing has significant influence. The ellipsoid fuzz with different local structure shows a sharp drop in He penetrative power around 150 nm below the surface. This is explained by how the ellipsoids are distributed over the depth of the system, see fig. 7. For the first  $\sim 100$  nm below the surface the ellipsoid fuzz with different local structure has below average density while this is compensated by a very sharp spike in density from 150-170 nm.

In the absence of strong density variations, the He penetrative power shows an exponential decline with depth. Fig. 11 shows exponential fits to the curves for the original and textured systems.

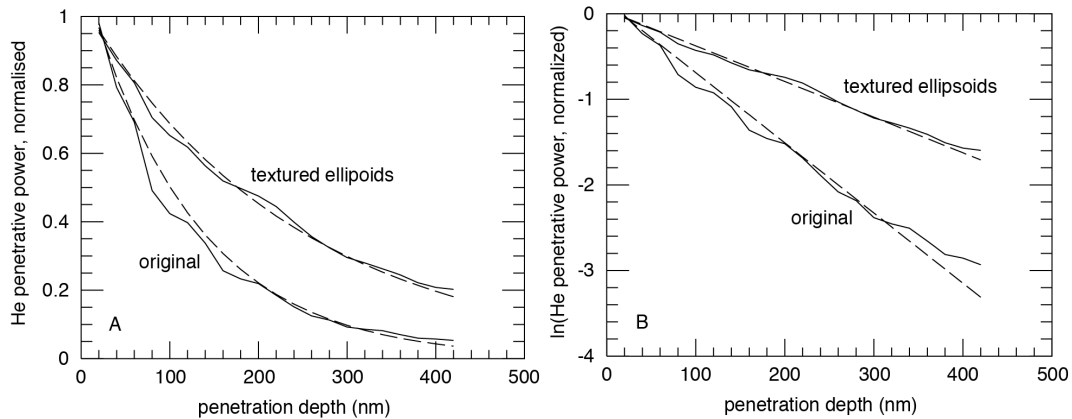


Fig. 11. He penetrative power as a function of penetration depth with exponential fits for the original and textured structures. The 0-20 nm range of the penetration depth has been excluded from the fit because the W density increases from 0 to 15vol% in this range, which does not result in an exponential decay pattern. A: linear scale. B: logarithmic scale.

Since penetrative power follows an exponential decay pattern, it can be described by a 'half depth'. For the original system the half depth is  $0.09 \mu\text{m}$ , for the textured system the half depth is  $0.18 \mu\text{m}$ .

#### 4.3 Thermalized He

Fig. 12 shows the concentration of thermalized He inside W (including He inside cavities) as a function of penetration depth.

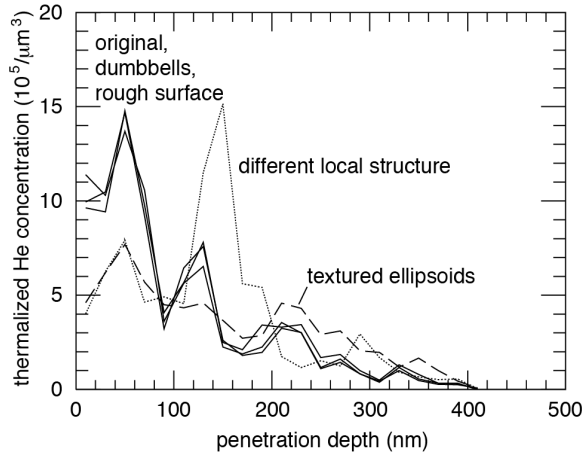


Fig. 12. Thermalized He concentration as a function of penetration depth for the five fuzz structures.

At first glance the thermalized He profiles in fig. 12 look quite different from the He penetrative power data shown in fig. 10. However, on closer inspection the two figures show roughly the same. The thermalized He concentration profiles are very sensitive to W density variations. However, the profiles for the original system, the dumbbells system and the system with a rough surface are again very similar, as in fig. 10. This shows that the spikiness in fig. 12 is not noise but a real influence of the W density distribution. Where the system with a different local structure has a steep decline in He penetrative power 150 nm below the surface due to a spike in W density around that depth, it has a sharp peak in thermalized He concentration at the same depth because many He ions will run into W surfaces there. Finally the textured ellipsoids system shows a more gradual decline of the thermalized He concentration with penetration depth than the original system, as was the case for the He penetrative power.

All thermalized He concentration profiles in fig. 12 virtually vanish beyond 400 nm penetration and there are drops in thermalized He concentration near the surface that deviate strongly from the exponential decaying pattern. This is because the W density near the surface and bottom varies gradually between 0 and the 15vol% average. There are fewer ellipsoids or dumbbells near the surface and bottom for He to run into and get trapped in. These deviations are therefore not an indication against the exponential decay pattern, but are instead a reflection of an uneven W density distribution.

#### 4.4 Transmitted He

Fig. 13 shows the angular distribution of He atoms that are transmitted through the fuzz layers.

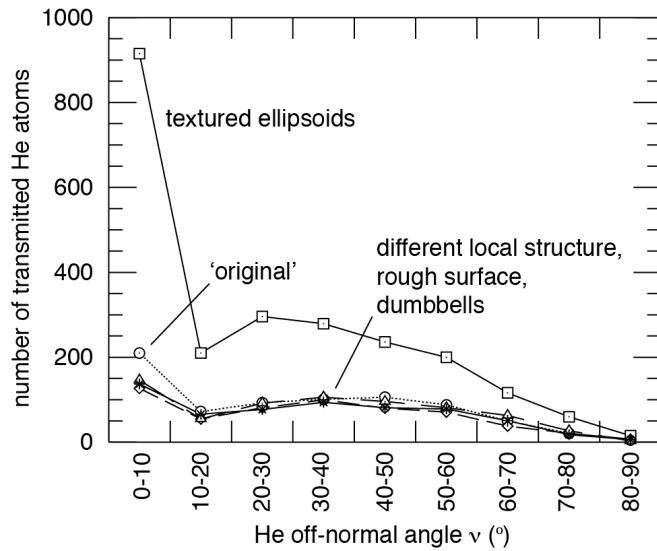


Fig. 13. Exit angular distribution of transmitted He atoms for the five fuzz structures.

It is clear from fig. 13 that the He atoms quickly lose their initial direction as they move through the fuzz. While the 0-10° bracket (which contains the 0-7° off-normal initial angles of the He ions) contains the highest number of He atoms for all fuzz structures, it represents only 22-28% of transmitted He atoms for the non-textured fuzz structures and 39% for the textured structure. After passing through 0.43  $\mu\text{m}$  of fuzz, a majority of transmitted He atoms have directions determined by previous bounces off W surfaces rather than still retaining their initial directions. Apart from the high He number in the 0-10° range and the remarkably low He number in the 10-20° range, the He transmission through these structures behaves as He vapour emerging from an open tube effusion cell with a radius/height ratio of  $\sim 1$ . The angular pattern is a slightly modified  $\cos(\nu)$  function [40]

#### 4.5 Reflected and outgassed He

Fig. 14 shows the number of He atoms that reflected or outgassed back to the vacuum as a function of the kinetic energy with which they reflected or outgassed.

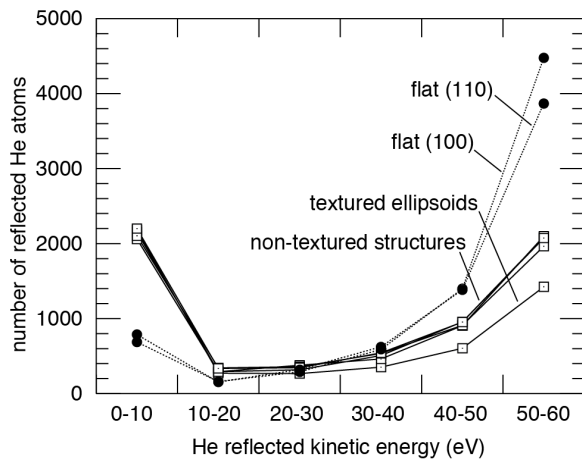


Fig. 14. Number of reflected or outgassed He atoms (out of 10000 impacts) as a function of the kinetic energy with which they reflected or outgassed. Open square data points connected by solid lines represent the five fuzz structures. The 0-10 eV bracket includes He atoms still flying freely through the fuzz with less than 8 eV kinetic energy at the end of the simulation and He atoms that outgassed from the bottom of the system (since in a real fuzz structure these would eventually have outgassed back to the vacuum). Transmitted He atoms were not included. Also shown, with solid circular data points connected by dotted lines, are the numbers of He ions that reflected off flat W (100) and (110) surfaces after 10000 impacts of 60 eV He.

Unsurprisingly, He atoms reflect off flat surfaces with a higher average kinetic energy than from fuzz structures. This is because He atoms reflect off flat surfaces after just one bounce, while many He atoms will bounce off multiple surfaces, losing kinetic energy with each bounce, before reflecting or outgassing back to the vacuum. This is in agreement with experiments by Takamura *et al* [41], who interpreted the lower reflected He energy from fuzz surfaces as the result of multiple He-W collisions.

#### 4.6 Recoil interaction approximation results

Fig. 15 shows the distribution of thermalized He inside normal W and inside crystalline bcc and amorphous W with larger interatomic distances, calculated in the recoil interaction approximation. The evenly spread density of the latter two is 14% of normal W, making the density in these calculations approximately the same as the overall density in the fuzz systems. The thermalized He distributions have been calculated by simulating 60 eV He impacts under 90° angle of incidence on W, using the MDRANGE code.

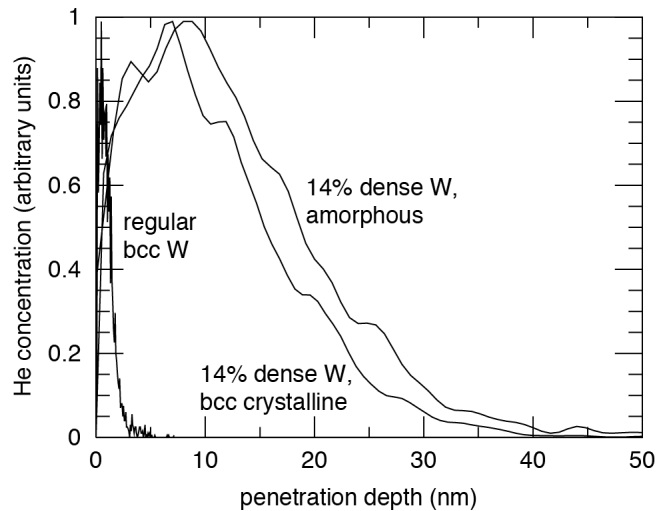


Fig. 15. Thermalized He distributions after 60 eV impacts on regular bcc W, on bcc W with a larger lattice parameter (14% density of normal W) and on amorphous W (14% density of normal W), calculated in the recoil interaction approximation.

Fig. 15 shows that few ions penetrate past 40 nm in the 14% dense systems, while for regular W the maximum He concentration lies at just 1 nm (the latter is in good agreement with He bombardment simulations on flat W carried out in LAMMPS, to obtain the flat surface data shown in fig. 14). The penetration depths for 14% dense systems are very different than for fuzz bombardment, where ~6% and ~23% of He ions penetrate through 0.43  $\mu\text{m}$  of non-textured and textured fuzz, respectively. This is because the results represent two qualitatively different phenomena. One represents He ions moving through a low, even W density. The other represents ions alternating between moving freely over some distance and then shortly penetrating a little into normal density W as they bounce off a surface, before moving on freely again.

A further demonstration that two calculations are qualitatively very different comes from the energy distributions of transmitted ions. The crystalline 14% density MDRANGE calculation was also run for a 20 nm thick foil. This value was chosen since at this thickness, about 10% of the ions were transmitted in the MDRANGE calculation, a percentage that is in between those for non-textured (6-7%) and textured (23%) fuzz systems. The results in fig. 16 show that the transmitted ion energy distributions are completely different, further highlighting that the nature of ion stopping is very different in the fuzz morphology.

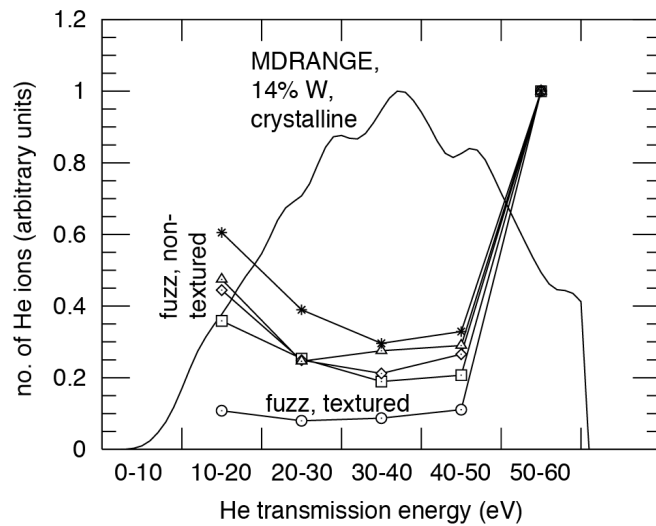


Fig. 16. He transmission energies for 0.43  $\mu\text{m}$  fuzz structures (MD) and a 20 nm bcc W foil (MDRANGE) with larger lattice parameter (14% density of normal W).

## 5 Discussion

It is clear that some of the parameters that were varied in the creation of fuzz structures have no significant effect on He ion penetration. This includes the unit building block shape and surface roughness. The question of which building block shape and degree of surface roughness is closest to experiment is not important here. The local arrangement of the ellipsoids has some influence if it makes a difference between having a relatively smooth W density distribution or strong density variations. In the system where the local structure was different, the regions of far below and far above average density caused a more gradual and steeper decline in He penetrative power, as expected. Deeper inside the fuzz with this different local structure, where the density distribution is similar to the original structure, the He penetrative power decreases with the same exponential pattern as in the original structure. The only parameter that makes a systematic big difference is the texturing of the ellipsoids, which increases the amount of open channels in the structure. Given that texturing of nanorods is sometimes clearly observed from experiments, the results of the textured system are probably closest to experiments.

At first glance the He penetration depths found would not seem to support the ballistic hypothesis very strongly. The textured system shows the deepest He penetration but even in that system He loses half its penetrative power in 0.18  $\mu\text{m}$ . From that, ballistic ion penetration could never adequately explain He penetrating through several  $\mu\text{m}$  of fuzz thickness that is reported in some experiments. However, the results represent a very conservative estimate for several reasons. By far the most important reason is that a very recent experimental determination of W fuzz density showed a decrease of a factor of nearly 3, from the originally reported  $\sim 10$  vol% to just 3.5 vol% [26]. Reducing the W volume in the simulations from 15 to 3.5 vol% would indeed greatly enhance He penetration by creating dramatically more open channels, see fig. 17.

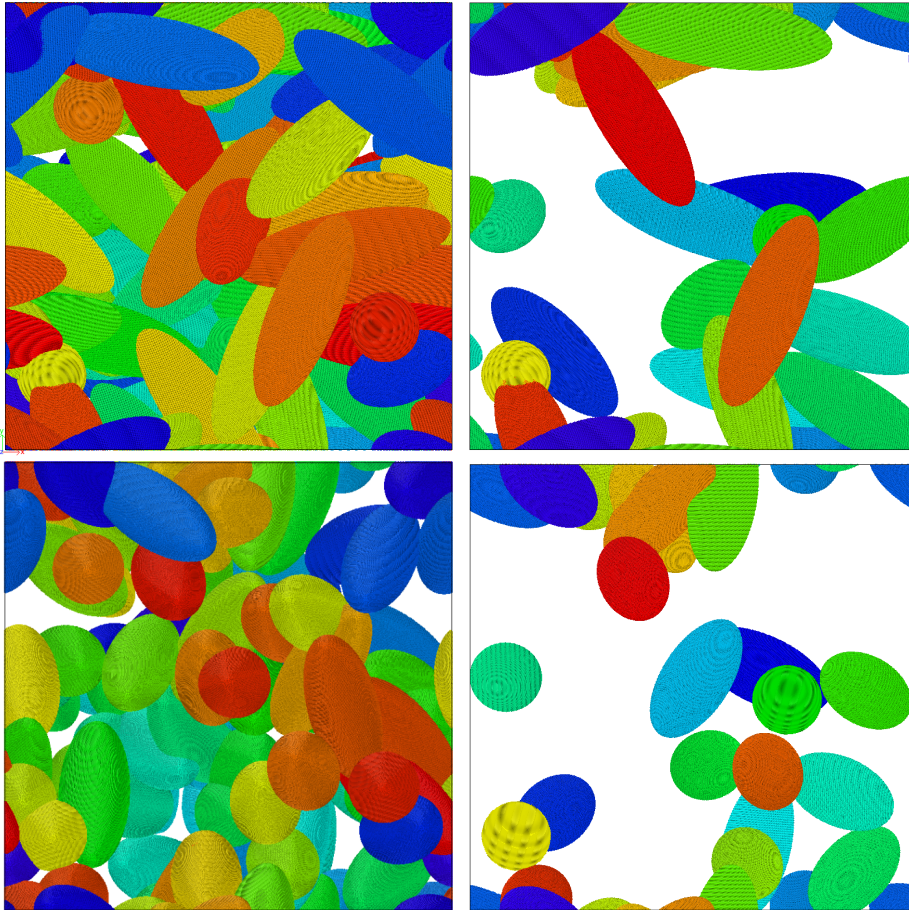


Fig. 17. Top views of the original and textured ellipsoid structures (top left and bottom left, 15 vol% W) and these same structures but with only every fourth ellipsoid shown (top right and bottom right, 3.7 vol% W).

For the original system in fig. 17, the amount of open channels increase from 0.4 to 37.4% when reducing the W density, while for the textured system it increases from 4.7 to 52.6%. Future work will include obtaining an accurate estimate of the half depth for lower density fuzz systems by redoing the calculations for lower density structures.

A second reason why He will penetrate deeper than shown in the current results is that the structures consisted only of 20 nm wide ellipsoids or dumbbells, while fuzz nanorods are up to 50 nm thick. Consolidating multiple smaller ellipsoids into bigger ones would result in a structure with a smaller silhouette in the direction perpendicular to the surface, and therefore more open channels, again increasing He penetration. Fig. 18 shows the top view of a 3.7 vol% non-textured fuzz structure, 2.34  $\mu\text{m}$  thick, built out of ellipsoids with different widths.





Fig. 18. Top view of a non-textured fuzz structure, 2.34  $\mu\text{m}$  thick and 0.2  $\mu\text{m}$  in-plane dimensions, built out of 20, 30, 40, and 50 nm wide ellipsoids.

The structure in fig. 18 has 5.0% open channels, comparable to the textured structure in the present work. Assuming that the open channel percentage is the sole governing factor for He penetration, the fuzz structure in fig. 18 might have a He penetration half depth over 1  $\mu\text{m}$ .

Finally, long-shaped nanorods with a degree of texture perpendicular to the surface might have a smaller silhouette still, because some of the bottom part of the nanorod would be hidden behind the top part, thus not blocking any more open channels. By contrast, the same amount of W spread out over multiple ellipsoids might block off multiple channels.

The smaller W density in recently reported experiments favours the ballistic scenario while it makes the idea of He diffusing through  $\sim 3$  times fewer nanorods yet more unlikely. The diffusion and ballistic penetration scenarios make different predictions for what happens after a very large exposure dose. Given that it is now established that He ions are capable of ballistically penetrating significant distances through fuzz towards the base of the fuzz growth, it can be determined, given some assumptions, whether the growth rates observed are compatible with this.

It is assumed that fuzz growth rates are in some way governed or limited by the amount of He which penetrates to the bottom of the fuzz structure. For example the limiting factor can be the formation (and migration) rate of new He bubbles in the main tungsten matrix. It can be proposed that this is the driving factor in growth, and that He bubble growth of the bubbles trapped within the nanorods plays a negligible role in this case. If this assumption is made then the growth rate of the fuzz is simply related to the He flux penetrating to the bottom of the layer ( $\Gamma_{bot}$ ), i.e.

$$\frac{dz}{dt} = A\Gamma_{bot} \quad (1)$$

where  $z$  is the fuzz thickness,  $t$  is time and  $A$  is a proportionality constant dependent on various physical parameters such as the material temperature, the ion energy and the thermophysical properties of the material related to bubble growth and migration, with units  $\text{m}^3$ .  $1/A$  can be described as a He density for a



given rate of growth. Taking the fact that the modeling shows that the He flux which reaches the base of the structure can be described by an exponential decay of the flux to the top of the structure ( $\Gamma_{top}$ ) (fig. 10) the height growth rate can thus be described as

$$\frac{dz}{dt} = A\Gamma_{top}e^{-z/z_0} \quad (2)$$

where  $z_0$  is the decay constant of the fuzz. Integrating both sides and solving for  $z$  thus gives

$$z = z_0 \ln \left( \frac{A\Gamma_{top}t}{z_0} + \frac{C}{z_0} \right) \quad (3)$$

where  $C$  is the integration constant. Given the generalized boundary condition that for  $t < t_0$   $z=0$  due to an incubation period for He bubble growth as proposed by Petty *et al* [26] it can be shown that for  $t \geq t_0$

$$z = z_0 \ln \left( \frac{A}{z_0} (\Phi - \Phi_0) + 1 \right) \quad (4)$$

where  $\Phi = \Gamma_{top}t$  is the fluence to the top of the fuzz and  $\Phi_0$  the incubation fluence. Taking the set of data used in [26] to derive an empirical  $(\Phi - \Phi_0)^{0.5}$  dependence, which was all at a similar surface temperature, it is possible to determine if this ballistic model is also a good fit to the same data set. A least squares fit to this data is shown in figure 19. This regression gives  $z_0 = 1.64 \pm 0.07 \mu\text{m}$ ,  $1/A = 3.23 \pm 0.20 \cdot 10^{19} \text{ particles m}^{-3}$  and  $\Phi_0 = -0.0045 \pm 0.0060 \cdot 10^{26} \text{ particles m}^{-2}$ . For  $\Phi_0$  this result is clearly unphysical, but the errors are large enough to provide for a small positive result. Another least squares fit holding  $\Phi_0=0$  gives a good fit with similar results of  $z_0 = 1.61 \pm 0.06 \mu\text{m}$ ,  $1/A = 3.11 \pm 0.14 \cdot 10^{19} \text{ particles m}^{-3}$  indicating an incubation fluence may not even be necessary in this case. It should also be noted that the data used here is that corrected for mass gain/loss in [26], but the use of uncorrected data gives very similar values ( $z_0 = 1.49 \pm 0.05 \mu\text{m}$ ,  $1/A = 2.93 \pm 0.12 \cdot 10^{19} \text{ particles m}^{-3}$ ). In all cases the normalized  $\chi^2$  is in the range 11-12, (versus  $\sim 15$  for the  $(\Phi - \Phi_0)^{0.5}$  fit) which can give reasonable confidence in the result given the spread in the data. Overall therefore, it is possible to account for the observed growth rates entirely through the assumed dependence on flux to the fuzz base. The fit also makes a prediction for the exponential decay constant which is comparable to the half depth in the ballistic penetration model if the density is extrapolated to similar fuzz densities of 3.5 % as was recently found, again in [26].

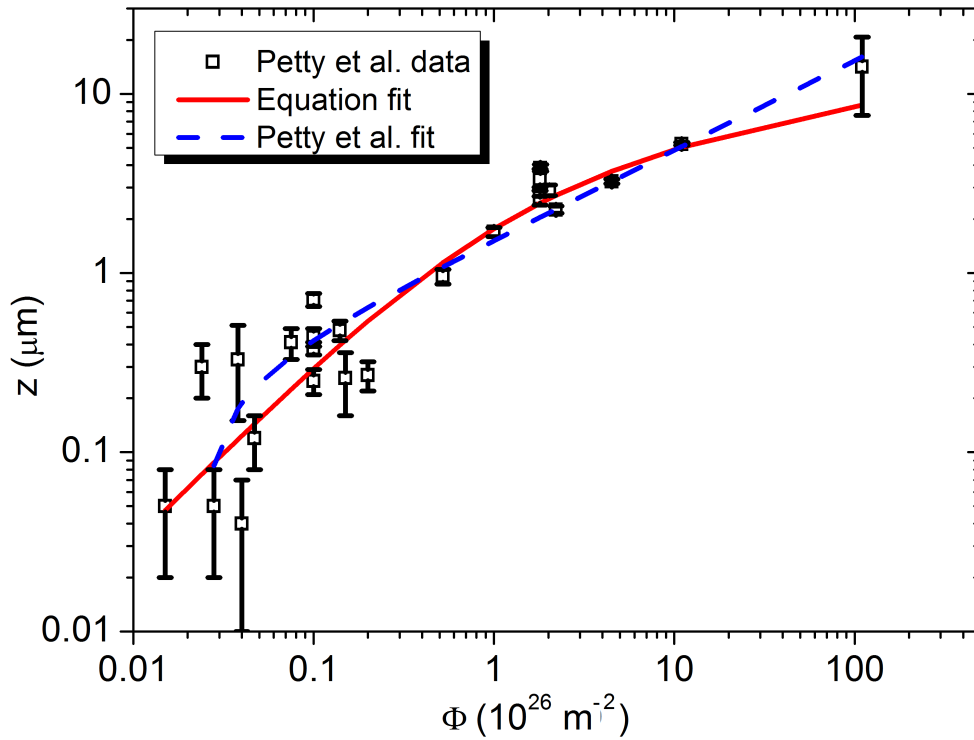


Fig. 19. Fuzz layer thickness as a function of fluence, with fits of  $(\Phi - \Phi_0)^{0.5}$  (blue dashed line) and eqn. 4 (red solid line). The experimental data and original fit are from [26].

## 6 Summary, conclusions and future directions

In a novel approach, large-scale MD simulations were performed of low energy He ion bombardment of ready-built W fuzz structures. The goal of the simulations was to see how deep He penetrates ballistically through fuzz and whether ballistic penetration could be a more realistic scenario than the (seemingly unlikely) scenario of He diffusing through the fuzz nanorods. Structures were built out of ellipsoidal or dumbbell-like pieces of bcc W, 20 nm wide. Fuzz layers were 0.43  $\mu\text{m}$  thick, had 15 vol% W, and consisted of up to 37 million atoms. To work around the limited experimental knowledge of the three-dimensional structure of fuzz, the structures were varied in several ways to see how these variations influence He penetration. Of the varied parameters, only the texturing of ellipsoids perpendicular to the surface had significant influence. This is because texture of the ellipsoids increases the amount of open channels through which He ions can travel unimpeded into the fuzz. Even with more open channels in the textured system, the majority of He ions have lost their initial direction after passing through 0.43  $\mu\text{m}$  of fuzz. In the absence of strong W density variations the He penetrative power decreases exponentially with depth. For the system of textured ellipsoids the half depth was 0.18  $\mu\text{m}$ . While this value already clearly shows that ions not only interact with the outer few dozen nm of the fuzz, the value is too small to explain He reaching the W bulk through

several  $\mu\text{m}$  of 15 vol% fuzz. However, in recently reported much sparser fuzz of only 3.5 vol% W, the amount of open channels would be far greater, leading to much deeper penetration, with half depths reaching likely up to a  $\mu\text{m}$  or further. This would make ballistic penetration a likely mechanism to explain even the thickest fuzz layers grown today [26], while the downward adjustment of the fuzz density makes He diffusion through fuzz nanorods still more unlikely. Results for fuzz structures are very different from recoil interaction approximation calculations on W with an equally low but homogeneous density. Future work should obviously include simulations on sparser fuzz structures, built out of building blocks with varying thickness, to make a closer comparison to the recently reported sparser fuzz structures. A better improvement than just lowering the W density would be to determine the three-dimensional structure of a piece of fuzz, to act as better input for future simulations. To our knowledge the three-dimensional structure of fuzz has not been resolved yet. One might consider filling up most of the open space between the fuzz with a method like atomic layer deposition or by letting some very low-viscosity molten substance or chemical penetrate into the structure and then letting it solidify or chemically harden. This should make the fuzz structure cohesive enough for ion milling out a thin rod without the nanorods detaching. The three-dimensional structure of this rod could then hopefully be resolved through TEM tomography.

## Acknowledgements

This work was funded by the Stichting voor Fundamenteel Onderzoek der Materie (FOM), which is financially supported by the Nederlandse Organisatie voor Wetenschappelijk Onderzoek (NWO).

## Appendix A: Objections to the He diffusion limited fuzz growth model

The most important problem for He diffusing through fuzz nanorods to reach the W bulk is how any significant amount of He could reach the bulk without desorbing back to the vacuum.

Fuzz nanorods are reported as having thicknesses ranging from 10-50 nm near the surface and possibly somewhat greater thickness near the bottom of the fuzz layer [3, 7, 12, 4, 1]. Fuzz thicknesses reported in [26] reached up to 6.5  $\mu\text{m}$ . For such fuzz layers, the length to thickness ratio of a perfectly straight nanorod that runs from the outer fuzz surface to the W bulk would exceed 100:1. Interstitial He will readily desorb from W if it diffuses to a surface. Hence, much He would desorb from the nanorods while diffusing through them, as W surfaces would always be relatively close by and only those He atoms that always avoid diffusing near surfaces would reach the bulk. Apart from avoiding going near surfaces, interstitial He atoms should also avoid going into He bubbles present inside nanorods. While some He atoms may escape from bubbles again after being trapped in them, it is also possible that growing He bubbles inside nanorods would burst, releasing He to the vacuum. Even without He bubbles present, He interstitials would also need to avoid other He interstitials as they would cluster

together and then self-trap (see trapping energies quantified by Density Functional Theory by Boisse et al [42]) and immobilise, forming the nucleus of a new bubble.

While it could be argued that a small portion of a continuous He supply from the plasma might successfully diffuse through the nanorods without desorbing or getting trapped in a bubble that bursts to the vacuum, this assumes that uninterrupted pathways for diffusion are available. This seems doubtful for several reasons. Uninterrupted pathways for He diffusion should also allow heat conduction. However, modelling by Kajita et al [2, 18] suggests that thermal conductivity of W fuzz is orders of magnitude lower than that of bulk W, which is much lower than being proportional to the fuzz volume fraction. They have also explained [18] some of their findings in terms of thermally isolated parts in their fuzz structures. Additionally, there is the fear expressed by some that parts of fuzz nanorods would detach completely and end up as nanodust in the core plasma. Considerations about orders of magnitude lower thermal conductivity, thermally isolated parts within the fuzz structure and parts of the fuzz detaching are all incompatible with the notion of continuous diffusion pathways through fuzz to the bulk.

Finally it seems unlikely that He would start out at a high concentration in the outer few tens of nm of the fuzz and only diffuse deeper into the fuzz (towards parts with low He concentration) without clustering and bubble formation, then be diluted further by more than an order of magnitude when it diffuses from the fuzz into the bulk, and then at this very diminished concentration start having a profound transformational effect that it never had inside the fuzz nanorods.

In summary, while it may seem obvious to interpret the square root pattern originally reported by Baldwin and Doerner in terms of something analogous to diffusion-limited film growth, the idea of He diffusing through nanorods to the bulk has a sufficient number of problems to be considered unrealistic.

It should be noted that while there are strong doubts about the idea of He diffusing through  $\mu\text{ms}$  of fuzz nanorods, He diffusion through bulk W under the fuzz layer seems indispensable to explain some observations. Baldwin and Doerner [6] reported fuzz present on grain boundaries deep below the surface, while He ions with  $< 100$  eV kinetic energy only penetrate ballistically for a few nm.

## Appendix B: analysing He trajectories

The criteria used to determine what happened to He ions are listed in Table B1.

Table B1. Categories of what can happen to He ions inserted into the system and the criteria for the categories.  $E_p$  and  $E_k$  are the potential and kinetic energies at the last recorded stage of a He atom and  $E_{p,ave}$ ,  $E_{p,min}$ ,  $E_{p,max}$  and  $E_{k,ave}$ ,  $E_{k,min}$ ,  $E_{k,max}$  are the average, minimum and maximum potential and kinetic energies of the last 10 recorded stages (1 stage is 100 MD steps of  $\sim 0.047$  ps) of a He atom.

category	what happens to He	Criteria
reflected	He passes through top of box, after bouncing off one or more W surfaces, carrying away a	last recorded stage of the He atom is within $10 \text{ \AA}$ of the top of the box and $E_k > 8 \text{ eV}$

	significant amount of kinetic energy	
outgas from top	He passes through top of box, after bouncing off one or more W surfaces, having transferred most kinetic energy to the fuzz	last recorded stage of the He atom is within 10 Å of the top of the box and $E_k < 8$ eV
thermalized	He penetrates into a W surface and reaches thermal equilibrium, is confined to small volume of one or a few interstitial sites	in last 10 stages: - $E_{p,min} > 0$ eV - $E_{p,max} < 4$ eV - $E_{k,ave} < 1$ eV - $E_{k,max} < 2$ eV
thermalized, inside ellipsoid/ dumbbell cavity	He penetrates into a W surface and reaches the ellipsoid or dumbbell cavity	in the last 3000 stages, the He atom has bounced off a W surface at least six times and the He atom has not travelled further than the length of the cavity
free, high energy	He moves through open space with enough kinetic energy to potentially still penetrate into W	in last stage: - $E_p = 0$ - $E_k > 8$ eV
free, low energy	He moves through open space without sufficient kinetic energy to still penetrate into W	in last stage: - $E_p = 0$ - $E_k < 8$ eV
transmitted	He passes through the bottom of the system with enough kinetic energy to potentially still penetrate into W	last recorded stage of the He atom is within 10 Å of the bottom of the box and $E_k > 8$ eV
outgas from bottom	He passes through the bottom of the system without sufficient kinetic energy to still penetrate into W	last recorded stage of the He atom is within 10 Å of the bottom of the box and $E_k < 8$ eV

Determining if atoms have reflected, transmitted or outgassed is done without error. Despite having only information for He atoms available for analysis (unlike for He atoms, information for W atoms is not saved every 100 MD steps), determining which atoms have thermalized worked almost without error with the energy threshold values in Table B1. Distinguishing between free He atoms bouncing between W surfaces and He atoms trapped inside cavities was more difficult. To determine threshold values for the number of bounces of the He atom and the number of last steps in the trajectory used (3000) to make the distinction, it was first recorded from visualisation of trajectories what happened to 321 atoms that ended up in a cavity or remained free with low energy. Then the threshold values for the number of bounces and the number of last steps analysed was manually adjusted, to obtain the best match in an automated analysis. Applying the automated analysis process with these optimised parameters to 403 other trajectories of He atoms that remained free or were trapped in cavities, gave a 96% correct determination. While the threshold values of the number of bounces and the number of steps at the end of

the trajectory analysed could certainly be further improved and additional criteria could be used to improve the accuracy of the analysis, the current criteria and parameters in them are good enough for present purposes. In 0.16% of cases the criteria failed to make any determination of what happened to He atoms. In these cases a determination was made manually (if possible) from visual inspection of the trajectory.

The kinetic energy limit of 8 eV for determining which free He atoms could still penetrate into W was set to the W surface barrier for He atoms. Experimental results have suggested different energies for the surface barrier. In 2003 Nishijima et al [43] suggested it is between 12 and 18 eV. In 2004 the same authors presented results [44] showing that 5 eV should already be sufficient for some He ions to penetrate W. In 2006 three of the same authors and Kajita [1] showed fuzz formation from 12 eV He ions. It was assumed that He will not penetrate W anymore if it has less than 8 eV kinetic energy. Given the different experimental values, the value of 8 eV might be wrong by several eV. However, the results are not very sensitive to how high the surface barrier energy is set.

## References

\* klaver2@gmail.com

- 1 S. Takamura, N. Ohno, D. Nishijima, S. Kajita, Plasma Fusion Res. 1 (2006) 051
- 2 S. Kajita, S. Takamura, N. Ohno, D. Nishijima, H. Iwakiri, N. Yoshida, Nucl. Fusion 47 (2007) 1358
- 3 M. J. Baldwin, R. P. Doerner, Nucl. Fusion 48 (2008) 035001
- 4 S. Kajita, W. Sakaguchi, N. Ohno, N. Yoshida, T. Saeki, Nucl. Fusion 49 (2009) 095005
- 5 M. J. Baldwin, R. P. Doerner, D. Nishijima, K. Tokunaga, Y. Ueda, J. Nuc. Mater. 390–391 (2009) 886
- 6 M. J. Baldwin, R. P. Doerner, J. Nuc. Mater. 404 (2010) 165
- 7 S. Kajita, N. Yoshida, R. Yoshihara, N. Ohno, M. Yamagiwa, J. Nuc. Mater. 418 (2011) 152
- 8 Y. Ueda et al, J. Nuc. Mater. 415 (2011) S92
- 9 D. Nishijima, M. J. Baldwin, R. P. Doerner, J. H. Yu, J. Nuc. Mater. 415 (2011) S96
- 10 M. J. Baldwin, T. C. Lynch, R. P. Doerner, J. H. Yu, J. Nuc. Mater. 415 (2011) S104
- 11 R. P. Doerner, M. J. Baldwin, P. C. Stangeby, Nucl. Fusion 51 (2011) 043001
- 12 G. De Temmerman, K. Bystrov, J. J. Zielinski, M. Balden, G. Matern, C. Arnas, L. Marot, J. Vac. Sci. Technol. A 30 (2012) 041306
- 13 G. M. Wright, D. Brunner, M. J. Baldwin, R. P. Doerner, B. Labombard, B. Lipschultz, J. L. Terry, D. G. Whyte, Nucl. Fusion 52 (2012) 042003
- 14 S. Kajita, N. Yoshida, R. Yoshihara, N. Ohno, T. Yokochi, M. Tokitani, S. Takamura, J. Nuc. Mater. 421 (2012) 22
- 15 S. Kajita, T. Yoshida, D. Kitaoka, R. Etoh, M. Yajima, N. Ohno, H. Yoshida, N. Yoshida, Y. Terao, J. Appl. Phys. 113 (2013) 134301

- 16 G. De Temmerman, K. Bystrov, R. P. Doerner, L. Marot, G. M. Wright,  
K. B. Woller, D. G. Whyte, J. J. Zielinski, J. Nuc. Mater. 438 (2013) S78
- 17 S. Kajita, N. Ohno, M. Yajima, J. Kato, J. Nuc. Mater. 440 (2013) 55
- 18 S. Kajita, G. De Temmerman, T. Morgan, S. van Eden, T. de Kruif, N. Ohno,  
Nucl. Fusion 54 (2014) 033005
- 19 O. El-Atwani, S. Gonderman, M. Efe, G. De Temmerman, T. Morgan,  
K. Bystrov, D. Klenosky, T. Qiu, J. P. Allain, Nucl. Fusion 54 (2014) 083013
- 20 T. J. Petty, J. W. Bradley, J. Nuc. Mater. 453 (2014) 320
- 21 K. B. Woller, D. G. Whyte, G. M. Wright, J. Nuc. Mater. 463 (2015) 289
- 22 G. M. Wright, G. G. van Eden, L. A. Kesler, G. De Temmerman, D. G. Whyte,  
K. B. Woller, J. Nuc. Mater. 463 (2015) 294
- 23 Y. Noiri, S. Kajita, N. Ohno, J. Nuc. Mater. 463 (2015) 285
- 24 O. El-Atwani, S. Gonderman, S. Suslov, M. Efe, G. De Temmerman,  
T. Morgan, K. Bystrov, K. Hattar, J. P. Allain, Fusion Eng. Des. 93 (2015) 9
- 25 D.U.B. Aussems, D. Nishijima, C. Brandt, H. J. van der Meiden, M. Vilémová,  
J. Matějček, G. De Temmerman, R. P. Doerner, N. J. Lopes Cardozo, J. Nuc.  
Mater. 463 (2015) 303
- 26 T. J. Petty, M. J. Baldwin, M. I. Hasan, R. P. Doerner, J. W. Bradley, Nucl.  
Fusion 55 (2015) 093033
- 27 S. Takamura, Y. Uesugi, Appl. Surf. Sci. 356 (2015) 888
- 28 S. Kajita, Y. Tsuji, N. Ohno, Phys. Lett. A 378 (2014) 2533
- 29 I. Tanyeli, L. Marot, M. C. M. van de Sanden, G. De Temmerman, ACS Appl.  
Mater. Interfaces 6 (2014) 3462
- 30 A.M. Ito, A. Takayama, Y. Oda, T. Tamura, R. Kobayashi, T. Hattori,  
S. Ogata, N. Ohno, S. Kajita, M. Yajima, Y. Noiri, Y. Yoshimoto, S. Saito,  
S. Takamura, T. Murashima, M. Miyamoto, H. Nakamura, Nucl. Fusion 55  
(2015) 073013
- 31 S. Takamura, T. Miyamoto, N. Ohno, Nucl. Fusion 52 (2012) 123001
- 32 S. Plimpton, J. Comput. Phys. 117 (1995) 1
- 33 N. Juslin, B. D. Wirth, J. Nuc. Mater. 432 (2013) 61
- 34 A. Stukowski, Model. Simul. Mater. Sci. Eng. 18 (2010) 015012  
<http://ovito.org/>.
- 35 K. Nordlund, Comput. Mater. Sci. 3 (1995) 448
- 36 J. Sillanpää, J. Peltola, K. Nordlund, J. Keinonen, M. J. Puska, Phys. Rev. B 63  
(2001) 134113
- 37 G. Hobler, G. Betz, Nucl. Instr. Meth. Phys. Res. B 180 (2001) 203
- 38 J. F. Ziegler, J. P. Biersack, U. Littmark, in: The Stopping and Range of Ions  
in Matter, Pergamon, New York, 1985
- 39 J. E. Valdés, C. Parra, J. Díaz-Valdés, C. D. Denton, C. Agurto, F. Ortega,  
N. R. Arista, P. Vargas, Phys. Rev. A 68 (2003) 064901
- 40 J. E. Mahan, Physical vapor deposition of thin films, Wiley, New York, 2000,  
ISBN 0-471-33001-9, p124
- 41 S. Takamura, S. Ono, N. Ohno, Contrib. Plasma Phys. 54 (2014) 474
- 42 J. Boisse, C. Domain, C. S. Becquart, J. Nuc. Mater. 455 (2014) 10
- 43 D. Nishijima, M. Y. Ye, N. Ohno, S. Takamura, J. Nuc. Mater. 313–316  
(2003) 97
- 44 D. Nishijima, M. Y. Ye, N. Ohno, S. Takamura, J. Nuc. Mater. 329–333  
(2004) 1029